We thank the reviewers for the comments that would undoubtedly improve the manuscript. We have carefully considered the reviewers' comments. The revised parts of the manuscript are given in red font.

Reviewer #1 (about your comments).

Comments and Suggestions for Authors

The authors have used three cameras operating at different wavelengths to measure the environmental radiation energy at each wavelength region to properly discuss the cause of the heat load.

The review paper will be improved if the following problems are solved.

1. Abstract

Significant results should be included in this section. Moreover, some suggestions after the pointed common conclusion are expected.

Response

We revised the sentences in the abstract to emphasize the difference from other studies and to mention the future potential from the results of this study.

Revised part

P.1

Abstract: In urban environments, radiation energy from the sun becomes a heat load on the human body. The radiation energy can be divided into visible, near-infrared, and far-infrared wavelengths. Far-infrared radiation is re-emitted from structures that have been warmed by the sun. On the other hand, visible and near-infrared light comes directly or reflected from structures. However, previous studies have measured environmental changes using only far-infrared cameras to study Urban Heat Island (UHI) countermeasures. Therefore, it is important to measure the environmental radiation energy at each wavelength region to properly discuss the cause of the heat load. To conduct the measurements, we used three cameras operating at different wavelengths, visible, near-infrared, and far-infrared. In addition, the measurements were conducted in different urban locations, seasons, and weather conditions in the Tokyo area of Japan, an urban metropolis. The results for far-infrared wavelengths show that in summer when the temperature is high, all structures except the sky have a positive heat load on the human body, while in winter or cloudy weather when the temperature is low, the heat load on the human body is negative. The results of heat load measurements at visible and near-infrared wavelengths show that the heat load varies greatly depending on the proportion of sky, plants, and buildings, despite the proportion of ground area being the same. These results indicate that the differences in radiation wavelengths need to be considered when considering reducing the heat load on the human body in urban environments. Therefore, the proposed method could contribute to the development of more effective UHI countermeasures by measuring in a various environments and countries.

2. Conclusions

Conclusions are given for summer, winter and cloudy days. Maybe some readers are very curious about rainy days in southern China or Kyushu area in Japan.

Response

In the conclusion, we revised the sentences to make it easier to understand what the results of this study will lead to in the future works. We hope that our results will enable us or readers to develop more effective measures of UHI, as the proposed methods can be used to make measurements in a variety of environments and countries.

Revised part

P.15

In this study, we propose a method to investigate the effects of the heat load or heat radiation energy from environmental structures on the human body, using three cameras at different wavelength ranges (visible light, near-infrared light, and far-infrared light). To demonstrate the usefulness of the method, the heat load from environmental structures to the human body was measured/determined under different seasons and weather conditions at different urban locations in Tokyo, Japan. The environmental structures were classified into four main categories; sky, plants, ground, and reaming structures such as buildings. The heat load by defining them to have positive value was evaluated individually from each environmental structure to the human body.

The measurements were conducted for the urban environment at three locations in Japan: The Imperial Palace, Ginza, and Daimon, where many people gather. The results of the structure classification showed that the percentage of ground remained almost the same at all locations, while the percentage of structures other than the ground changed.

Summer season measurements showed that structures other than the sky at far-infrared wavelengths exert a positive heat load on the human body. Therefore, considering only at the far-infrared wavelengths, the larger the sky area, the smaller the heat load on the human body. On the other hand, a positive heat load was given from the sky to the human body in the visible and near-infrared wavelengths. In addition, the heat load from the ground to the human body varied greatly even if the area of the ground remained unchanged. As the area of the plants increased, the radiation to the ground was shielded and the heat load from the ground to the human body decreased. However, as the area of the buildings increased, the heat load from the ground also increased.

Winter season measurements showed that the heat load became negative for all structures in the far-infrared wavelengths. On the other hand, all heat loads were smaller at visible and near-infrared wavelengths because the flux of sunlight reaching the ground surface was smaller. Therefore, the negative heat load in the far-infrared was dominant in winter, and the visible and near-infrared radiation had little effect on the heat load to the human body.

Cloudy weather measurements showed that the heat load from the ground at visible and near-infrared wavelengths almost disappeared, and the heat load from the sky became dominant. Due to the cloudy weather and the seasonal difference from the summer experiment, the temperature of all structures was

lower than that of the human body, and they showed negative heat loads in the far-infrared wavelengths, as in winter.

These results indicate that the heat load on the human body due to radiation at visible, near-infrared, and infrared wavelengths varies in a complex manner depending on the proportion of city structures and variations from season and weather. In this experiment, characteristic locations in Tokyo, Japan were chosen, but measurements can be realized in fact, by extending the proposed method to a wider variety of environments over different countries. We believe the findings reported in this paper could have implications when considering the countermeasures against UHI.

3. Future research suggestion

The selected three typical locations are good. However, only one static person is concerned which is not common situation. In future more dynamic people should be included for evaluation.

Response

In this case, the measurements were taken in a situation where few people were in the picture. As you pointed out, it will be interesting to measure in a crowded environment and to include people as one of the classifications in the analysis or evaluate the more dynamic people. We hope that the method proposed here can be used for measurements in various environments in the future work. We revised the conclusion to include the previous your comment and to mention future work.

Reviewer #2.

Comments and Suggestions for Authors

The manuscript is well written. However, there are some concerns that, if addressed suitably, can significantly improve the overall quality of the work. Some suggestions can be implemented, while the remainder can be considered as the scope of future work. For my detailed comment, please refer to the attached file.

In this paper, the authors have measured the radiation in visible, near infrared, and far infrared spectrum to analyse exchange of radiation between human body and urban environment. The authors have made the measurements at three different sites, The Imperial Palace, Ginza, and Daimon; all three sites are popular tourist spots located in Japan. The measurements are also taken in three different seasons, summer, winter, and on a cloud day between summer and winter.

In the first part of the manuscript, the authors have clearly explained the mathematics behind the images captured by the camera and the thermal radiation in each spectrum. The authors have used these mathematical equations to convert and measure the camera images in three different spectra to calculate the human heat load. The images in each spectrum are further categorized into sky, buildings, plants, and ground. Heat load from each category is analysed based on the pictures taken at different conditions.

The manuscript is very well written. All the sections are well organized. I recommend accepting the manuscript after addressing the following concerns:

Major comments:

1. **Please discuss the uncertainty in the estimation of intensity in three different spectra based on the camera specifications.**

Response

In this calibration experiment, to reduce the effects of variation of light source and camera pixel on the calibration experiments, we determined to use the central area of the captured image as the average value, as shown in the example in Figure A (Figure S1 in the supplementary file). Since the number of pixels for each camera was different, the number of pixels for the averaged area was also different. We added the detailed information in supplementary file, such as how many pixels were used for averaging. We also revised the results of the calibration experiment (Figures 2 and 4) in the manuscript to show the standard deviation as an error bar.

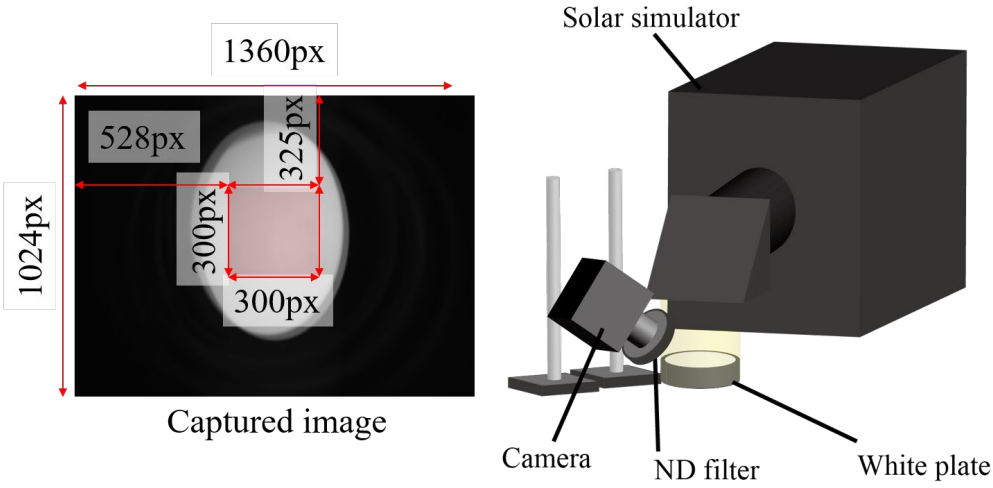

Figure A. Example of a measured image using standard diffuse reflector taken by a visible light camera, where the red area is obtained as the average value.

Revised part

P.4

The measurement results of this calibration experiment are shown in Figure 2. The vertical axis shows the raw data of the camera luminance data D. The horizontal axis, i, is the value taken with respect to i_{dr}, the value obtained by integrating equation (3) over the wavelength range in which each camera can measure. The plotted data is the averaged value of the central area of the diffuse reflector, and the error bars are its standard deviation. This averaging process is detailed in the supplementary file (Section A). As can be seen from the graph, the luminance data D obtained by the cameras decreases as the light intensity is reduced by the ND filters.

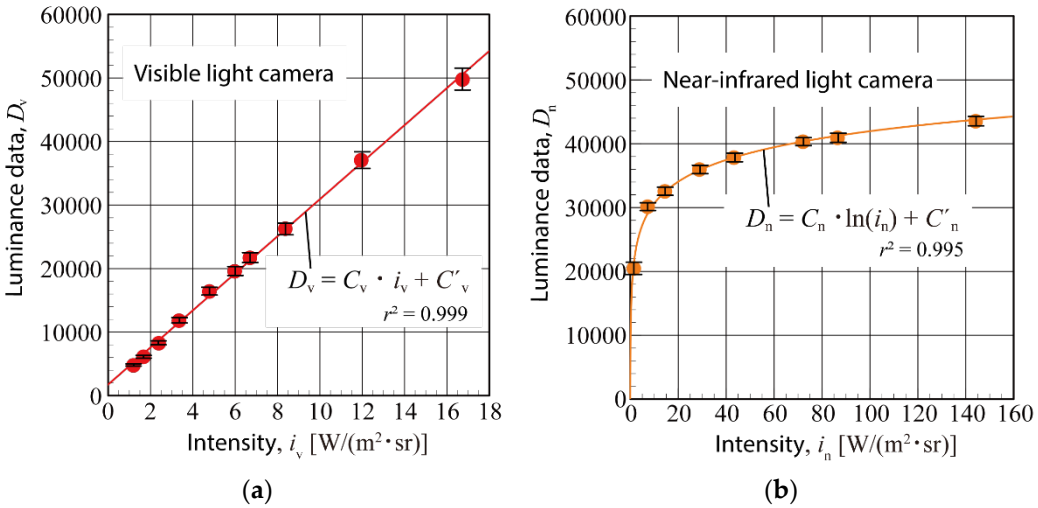

Figure 2. Measurement results for calibration experiment of (a) visible light camera and (b) near-infrared light camera.

P.6

Figure 4 shows the measured luminance data $D_{f,b}$ as a function of the heat exchange between the two black bodies represented by $\sigma(T_b^4 - T_s^4)$ with the camera sensor temperature being T_s. The plotted data is the averaged value of the central area of the blackbody sample, and the error bars are its standard deviation. This averaging process is detailed in the supplementary file (Section A). The measured irradiance data has a linear relationship with the exchanged radiation energy with the coefficients C_f and C'_f for the linear approximation. The determination of these coefficients were calculated by the least-squares method.

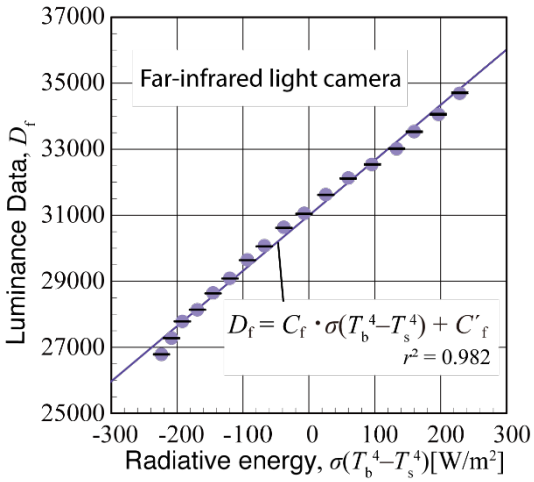

Figure 4. Data stored in far-infrared light camera versus measured radiative energy.

2. In Fig.7, were all the pictures in three spectra taken from 1.7 m height from the ground level? If so, discuss the orientation of the camera with respect to the ground surface as this could significantly change the contribution from sky and other categories.

Response

There was a lack of information on how to set up the camera and acquire images, so we added detailed information as a supplementary file.

As shown in Figure B below (Figure S2 in the supplementary file), the camera height from the ground level was standardized to 0.92 m for all cameras. This camera height was determined based on setting the center point of the coordinate axis at 0.54h defined by Dunkel et al. [29] which was used as a reference for the view factor equation (Eq. 9). Although it was mentioned in Figure 5, there was not enough text to explain it in the manuscript, so we revised the height setting to be mentioned in the text as well.

The camera was equipped with a mechanical unit that could rotate horizontally and vertically, and the camera was oriented so that it could capture images from the ground to the sky.

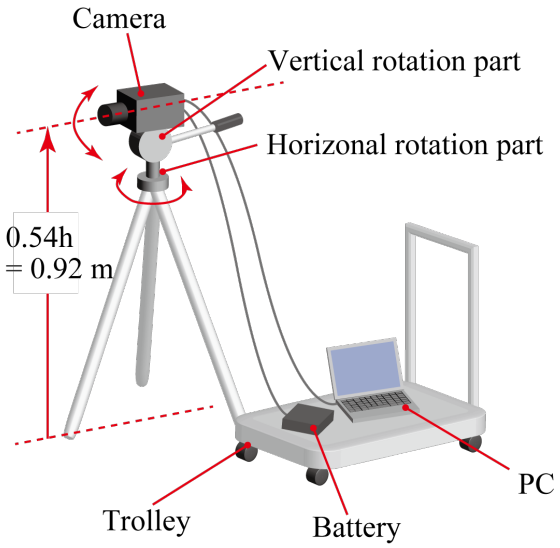

Figure B. Schematic diagram of measurement using a camera attached with a rotation unit

Revised part

P.7

Dunkel et al. [30] measured view factor on a typical subject in various positions and derived the view factor equation between the standing person and their surroundings was derived. From the view factor derived by them, $F_{p\rightarrow hb}$ can be expressed by the following equation:

$$F_{p\rightarrow hb}=\frac{0.1386hw^{\frac{1}{3}}\left\{0.65+\cos\alpha\left|\left(0.715+0.52\left|\cos\varphi\right|\right)\right|\right\}\sqrt{x^2+y^2+z^2}}{(x^2+y^2+z^2)^{\frac{3}{2}}}, \quad (9)$$

where, assuming the height h = 1.7 m and the weight w = 70.0 kg to do the calculations in Section 3. The camera height from the ground level was fixed at 0.54h = 0.92 m. This camera height was determined based on the center point of the coordinate axis as shown in Figure 5 defined by Dunkel et al. [30]. A description of the equipment used to make measurements with each camera along this coordinate axis was given in supplementary file Section B.

3. For Eqs.4 and 5, please mention the statistical metrics for the least square method such as correlation coefficient and root mean square values.

Response

We added correlation coefficients (r^2) to the figure for all results of the least squares method.

Revised part

P.4

where, the C_v and C'_v are coefficients for linear approximation, and C_n and C'_n are coefficients for logarithmic approximation. The determination of these coefficients were calculated by the least-squares method. The correlation coefficient r^2 was shown in each figure.

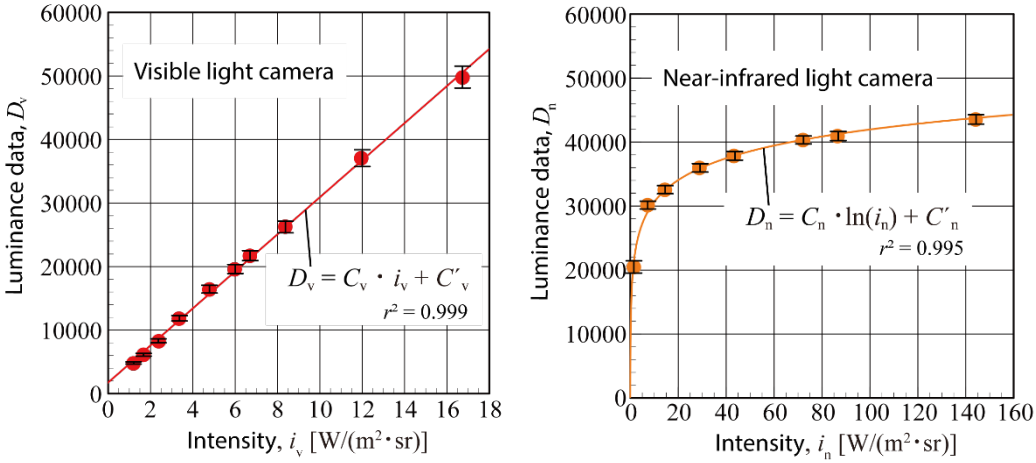

Figure 2. Measurement results for calibration experiment of (a) visible light camera and (b) near-infrared light camera.

P.6

Figure 4 shows the measured luminance data $D_{f,b}$ as a function of the heat exchange between the two black bodies represented by $\sigma(T_b^4 - T_s^4)$ with the camera sensor temperature being T_s. The plotted data is the averaged value of the central area of the blackbody sample, and the error bars are its standard deviation. This averaging process is detailed in the supplementary file (Section A). The measured irradiance data has a linear relationship with the exchanged radiation energy with the coefficients C_f and C'_f for the linear approximation. The determination of these coefficients were calculated by the least-squares method. The correlation coefficient r^2 was shown in the figure.

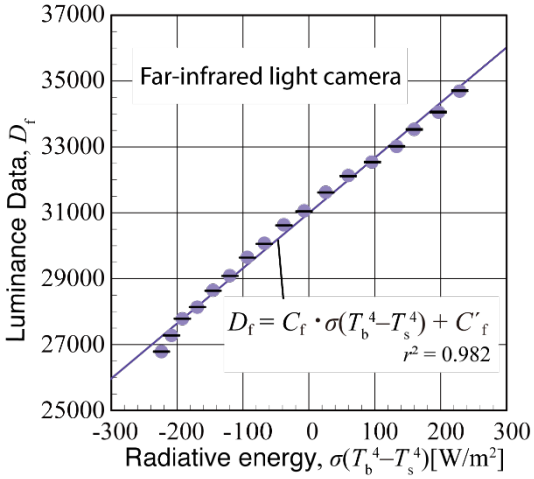

Figure 4. Data stored in far-infrared light camera versus measured radiative energy.

4. **Tables 1, 2, and 3: Please mention at what time the measurements were taken as it could be a significant factor for discussion. The orientation of Sun based on local time could result in shadow effect from the nearby buildings or canopy, and hence affect the heat load. It is not clear if this factor is included in the present analysis. The authors can however consider this as future scope of the work, if they feel irrelevant for the present study.**

Response

We revised the table to include the time at each measurement. The experiment started at the same time (12:00 noon) at each location. In addition, to minimize the influence of time and weather changes on the measurements, the working time to obtain all images was to be less than one hour.

As you pointed out, the sun's orientation depends not only on the time of day, but also on the country, and the shadows created by the sun also change. We believe that once the method proposed in this manuscript is established, we can treat these factors as variables, and future measurements will precisely clarify what factors affect the heat load on the human body. We revised the discussion to mention it in the conclusion.

Revised part

P.8

Table 1. Environmental conditions of measurement location in summer experiments.

Location	Date	Temperature [°C]	Humidity [%]	Barometric Pressure [hPa]	Starting time of measurement
Ginza	Jul. 29, 2020	31.2	68	999.1	12:00 noon
Daimon	Aug. 4, 2020	32.8	63	1007.8	12:00 noon

Ginza	Aug. 19, 2020	33.0	55	1012.3	12:00 noon
The Imperial Palace	Aug. 26, 2020	34.9	65	1008.3	12:00 noon
Daimon	Aug. 27, 2020	32.2	63	1008.3	12:00 noon
The Imperial Palace	Aug. 30, 2020	31.8	64	1008.5	12:00 noon

p.12

Table 2. Environmental conditions of measurement location in winter experiment.

Location	Date	Temperature [°C]	Humidity [%]	Barometric pressure [hPa]	Starting time of measurement
The Imperial Palace	Feb. 4, 2020	12.2	26	1006.9	12:00 noon
The Imperial Palace	Feb. 5, 2020	9.9	38	1016.0	12:00 noon

p.13

Table 3. Environmental conditions of measurement location in cloudy weather.

Location	Date	Temperature [°C]	Humidity [%]	Barometric pressure [hPa]	Starting time of measurement
The Imperial Palace	Oct. 19, 2021	14.3	68	1013.2	12:00 noon
The Imperial Palace	Oct. 25, 2021	16.6	59	1021.4	12:00 noon

5. Is there any specific reason why the effect of winter and cloudy condition was studied only for one site, The Imperial Palace?

Response

To simplify the comparison with cloudy weather, we chose The Imperial Palace, where the sky is unsealed by buildings or plants. As stated in the response to the previous comment, we hope to clarify the relationship between the heat load and various other factors, such as changing the location other than The Imperial Palace and the time of day, using this method in future works. We revised the manuscript to include the reason for choosing the location as a comparison.

Revised part

p.12

3.2. Experiments under winter conditions

3.2.1. Measurement location and environmental conditions

As an experiment to compare the difference between summer and winter seasons, we conducted an experiment on a sunny day in February at the Imperial Palace, the same place where we conducted the investigation in summer. To simplify comparison with cloudy weather, The Imperial Palace, where the sky is not blocked by buildings or plants, was chosen. The conditions at the time of measurement were measured in the same way as in summer. The meteorological data are shown below in Table 2.

Minor comments:

1. **Page 2, L.No.94, 95: change the wavelength unit from um to μm.**

Response

We revised the unit for wavelength from um to μm in this manuscript.

2. **Page 3, L.No.101: Change "…radiation intensity and to know the…" to "radiation intensity to know the…".**

Response

We revised the sentence as you mentioned.

3. **Page 11, L.No.320: Change the Section 3.2 subheading to read as "Experiments under winter conditions".**

Response

The subheading was a typographical error. We revised the Section 3.2 subheading as you mentioned.

4. **Page 12, L.Nos.345 – 349: Split the long sentence into several short sentences for better readability.**

Response

We revised the sentence to make it more readable.

Revised part

p.13

The major changes when compared to the summer experiment was seen in the results of the far-infrared experiment. In summer, the temperature of all structures except the sky was higher than that of the human body, resulting in a positive heat load on the human body. In winter, however, the temperature of all structures was lower than that of the human body, resulting in a negative heat load. Furthermore, in the visible and near-infrared radiation, the radiation energy from the sky and ground were decreased. This is due to the fact that the angle of incidence of sunlight is larger in winter than in summer, and the flux of sunlight reaching the ground surface is smaller. A comparison focusing on the difference

in wavelengths showed that the negative heat load of far-infrared radiation was dominant in winter, while visible and near-infrared radiation energy had little effect on the heat load to the human body.

Reviewer #3.

Comments and Suggestions for Authors

General structure of paper is fine and it is well written. Paper is of current interest and falls in the scope of journal, however, there are following suggestions without addressing them paper should not be accepted for publication:

There are some typing errors in the manuscript. Please, check the paper again for any possible misprints

In the Abstract section, you should describe your work and contribution more clearly than what they were in the background of the research. Currently, it is hard to know the main content and results of this article from the Abstract.

The novelty should be further strengthened. It is not clear in the current manuscript.

The "Introduction" part is not well organized, although many references have been cited. The knowledge gap of the research topic was not reported. A good literature survey should be carefully prepared to show the aim of the study: whether to meet the knowledge gap or to uncover some novel findings. Based on the present introduction, one cannot easily judge the contribution of the present paper. To improve this section you can use "Usefulness of PCM in building applications focusing on envelope heat exchange–energy saving considering two scenarios"

The manuscript lacks a Nomenclature section. The relevant mathematical and Greek symbols must be identified alphabetically along with their units.

Response

We confirmed the typos and misprints, including the comments of other reviewers. We also revised and added sentences to the abstract and introduction of the manuscript to make it easier to convey the claims of our work. In the introduction, we organized the sentences to incorporate the reference you suggested, as it was good reference for our work as well.

We added Nomenclature section before Reference section.

P.1

> **Abstract:** In urban environments, radiation energy from the sun becomes a heat load on the human body. The radiation energy can be divided into visible, near-infrared, and far-infrared wavelengths. Far-infrared radiation is re-emitted from structures that have been warmed by the sun. On the other hand, visible and near-infrared light comes directly or reflected from structures. However, previous studies have measured environmental

changes using only far-infrared cameras to study Urban Heat Island (UHI) countermeasures. Therefore, it is important to measure the environmental radiation energy at each wavelength region to properly discuss the cause of the heat load. To conduct the measurements, we used three cameras operating at different wavelengths, visible, near-infrared, and far-infrared. In addition, the measurements were conducted in different urban locations, seasons, and weather conditions in the Tokyo area of Japan, an urban metropolis. The results for far-infrared wavelengths show that in summer when the temperature is high, all structures except the sky have a positive heat load on the human body, while in winter or cloudy weather when the temperature is low, the heat load on the human body is negative. The results of heat load measurements at visible and near-infrared wavelengths show that the heat load varies greatly depending on the proportion of sky, plants, and buildings, despite the proportion of ground area being the same. These results indicate that the differences in radiation wavelengths need to be considered when considering reducing the heat load on the human body in urban environments. Therefore, the proposed method could contribute to the development of more effective UHI countermeasures by measuring in a various environments and countries.

P.2

Many researchers are investigating and quantifying the UHI in various cities [9–18]. As a result, it was pointed out that the heat island effect is not only caused by the radiation from urban structures but also by the large amount of heat generated by vehicles, power plants, and air conditioners heating the atmosphere. The resulting increase in atmospheric temperature leads to increased energy consumption. To solve this problem, it is important to reduce energy consumption as much as possible. Kalbasi et al. [18] showed that energy savings can be realized when phase change material (PCM) was used for walls and ceilings by selecting the material appropriately in accordance with the local environmental conditions. In addition to these building insulation effects, there is also growing discussion on heat radiation, such as improving materials used in urban buildings and increasing vegetation to reduce solar heat re-radiation [10].

To realize a comfortable urban environment, it is necessary to understand the heat load to the human body caused by radiation in urban environments. Yamaguchi et al. [19] analytically evaluated the exchange of heat radiation between the outdoor environment and the human body, assuming a street space flanked by buildings and space with buildings on only one side. As a result, presence or absence of the structures strongly influenced the exchange of heat radiation between the human body and the surrounding environment. In addition, quantitative evaluations of the factors that contributed to a flux of heat radiation in the outdoor environments [20–24]. Yu et al. [25] used a far-infrared camera to measure the surface temperature of the environment from specific locations to quantify the sensible heat flux in the urban landscape. The surface temperatures of road, grassland, tree, wall, water, and air in the environment changed with time, and the maximum surface temperature of the wall exceeded 55°C in summer. In summer, the highest surface temperature of the wall was over 55°C. Especially, the wall and road temperature increased significantly, and the highest surface temperature was observed between noon and 2 pm.

In the study of UHI, quantitative investigations in the far-infrared wavelength range have been conducted to evaluate the temperature and radiation of structures heated by sunlight. However, of the total energy of sunlight calculated based on Planck function (temperature of sun T_{sun} assumed to be 5778 K), far-infrared light (wavelength λ above 2.5 μm) accounts for about 3.1%. In contrast, visible light (λ = 0.4 to 0.7 μm) and near-infrared light (λ = 0.7 to 2.5 μm) account for the remaining 36.7% and 47.7%, respectively. The far-infrared wavelengths of the heat load on humans are mainly due to the radiation emitted

from any structures, including the sky, plants, ground, or any other structures like buildings warmed by sunlight. On the other hand, visible and near-infrared radiation from the sun can reach humans directly, or after being reflected by any structures, so it is believed to have a significant impact on the exchange of heat between humans and the environment. Thus, the data obtained by the previous researchers [20–25], who have mainly studied the far-infrared wavelength range, are insufficient for analyzing the effects of radiation in each wavelength range on the UHI.

The radiation from the environment to the human body can be divided into the following three categories; (A) direct radiation from the sun to the human body, (B) radiation reflected or scattering by any structures, and (C) radiation from any warmed structures. Far-infrared measurements can only contribute to factors categorized in (C). Thus, we proposed a method for measuring visible, near-infrared, and far-infrared radiation from environments with the aim of investigating the effect of the radiation energy (A) to (C) on the exchange of heat between the human body and the environment. To demonstrate the usefulness of the proposed method, we performed measurement experiments using Charge Coupled Device (CCD) cameras under visible, near-infrared, and far-infrared wavelengths at different locations, seasons and weather conditions. The experiments revealed that the proposed method provides an overview of the effects of heat radiation in different wavelengths on the human body and could be a tool for characterizing the effects of heat radiation on human body.

P.16

Nomenclature

C, C'	:	approximation coefficients
D	:	luminance data
E	:	radiation flux, W/m^2
F	:	view factor
h	:	height of a person, m
i	:	radiation intensity, W/(m^2・sr)
N	:	number of pixels
Q	:	radiation energy, W
R	:	constant value
r	:	correlation coefficient
S	:	area, m^2
T	:	temperature, K
w	:	weight of a person, kg
x, y, z	:	coordinate, m
θ	:	polar angle, degrees
λ	:	wavelength, m
ρ	:	reflectivity
σ	:	Stefan-Boltzmann constant, W/(m^2・K^4)
φ	:	azimuth angle, degrees

Subscripts

b	:	black body
dr	:	standard diffuse reflector
f	:	far-infrared
ground	:	ground
hb	:	human body
n	:	near-infrared
obj	:	observed objects in environmental experiment

p : point
raw : raw image
s : camera sensor
sph : sphere image
sun : sun
v : visible